

# Forecasting influenza incidence as an ordinal variable using machine learning

Haowei Wang<sup>1,2</sup>, Kin On Kwok<sup>3,4,5</sup>, Steven Riley<sup>1,2,\*</sup>

<sup>1</sup> School of Public Health, Imperial College London, UK

<sup>2</sup> MRC Centre for Global Infectious Disease Analysis and Abdul Latif Jameel Institute for Disease and Emergency Analytics, Imperial College London, UK

<sup>3</sup> JC School of Public Health and Primary Care, The Chinese University of Hong Kong, Hong Kong Special administrative regions, China

<sup>4</sup> Stanley Ho Centre for Emerging Infectious Diseases, The Chinese University of Hong Kong, Hong Kong Special Administrative Region, China

<sup>5</sup> Hong Kong Institute of Asia-Pacific Studies, The Chinese University of Hong Kong, Hong Kong Special Administrative Region, China

\*Corresponding authors: Steven Riley, [s.riley@imperial.ac.uk](mailto:s.riley@imperial.ac.uk), School of Public Health, Imperial College London, Norfolk Place, London, W2 1PG

NOTE: This preprint reports new research that has not been certified by peer review and should not be used to guide clinical practice.

## Abstract

Many mechanisms contribute to the variation in the incidence of influenza disease, such as strain evolution, the waning of immunity and changes in social mixing. Although machine learning methods have been developed for forecasting, these methods are used less commonly in influenza forecasts than statistical and mechanistic models. In this study, we applied a relatively new machine learning method, Extreme Gradient Boosting (XGBoost), to ordinal country-level influenza disease data. We developed a machine learning forecasting framework by adopting the XGBoost algorithm and training it with surveillance data for over 30 countries between 2010 and 2018 from the World Health Organisation's FluID platform. We then used the model to predict incidence 1- to 4-week ahead. We evaluated the performance of XGBoost forecast models by comparing them with a null model and a historical average model using mean-zero error (MZE) and macro-averaged mean absolute error (mMAE). The XGBoost models were consistently more accurate than the null and historical models for all forecast time horizons. For 1-week ahead predictions across test sets, the mMAE of the XGBoost model with an extending training window was reduced by 78% on average compared to the null model. Although the mMAE increased with longer prediction horizons, XGBoost models showed a 62% reduction in mMAE compared to the null model for 4-week ahead predictions. Our results highlight the potential utility of machine learning methods in forecasting infectious disease incidence when that incidence is defined as an ordinal variable. In particular, the XGBoost model can be easily extended to include more features, thus capturing complex patterns and improving forecast accuracy. Given that many natural extreme phenomena, such as floods and earthquakes, are often described on an ordinal scale when informing planning and response, these results motivate further investigation of using similar scales for communicating risk from infectious diseases.

## 40 **Author Summary**

41 Accurate and timely influenza forecasting is essential to help policymakers improve influenza  
 42 preparedness and responses to potential outbreaks and allocate medical resources  
 43 effectively. Here, we present a machine learning framework based on Extreme Gradient  
 44 Boosting (XBoost) for forecast influenza activity. We used publicly available weekly  
 45 influenza-like illness (ILI) incidence data in 32 countries. The predictive performance of the  
 46 machine learning framework was evaluated using several accuracy metrics and compared  
 47 with baseline models. XGBoost model was shown to be the most accurate prediction  
 48 approach, and its accuracy remained stable with increasing prediction time horizons. Our  
 49 results suggest that the machine learning framework for forecasting ILI has the potential to  
 50 be adopted as a valuable public health tool globally in the future.

# Introduction

Influenza forecasting plays a critical role in helping healthcare planners and policymakers to improve response to large seasonal epidemics and to mitigate their impact in terms of morbidity and mortality as well as social and economic impacts. Before the COVID-19 pandemic, a contagious respiratory illness caused by influenza viruses posed continual threats globally, causing an estimated 1 billion cases and up to 650000 deaths annually [1,2]. Accurate and timely forecasting of influenza epidemics in terms of the start of the epidemic, the time and size of the peak, and the duration of the epidemic enable policymakers to take effective interventions and optimise the allocation of healthcare resources. For example, to conduct the maximum number of elective surgical procedures prior to opening up space in intensive care wards for community-acquired pneumonia patients. However, reliable influenza forecasts remain a substantial challenge due to the variation of dominant influenza strains and environmental factors affecting the outbreak intensity. [3–5].

Different analytical methods have been used as the basis for forecast models of influenza disease. These methods can be classified into two broad categories: mechanistic models and statistical methods [5–7]. Mechanistic models attempt to reproduce key features of the underlying mechanism of transmission. Typical examples include classic compartmental models [8–11] and agent-based models (ABMs) [12–15]. Statistical approaches are phenomenological and do not attempt to reproduce the transmission mechanism, such as autoregressive integrated moving average (ARIMA) [16,17] and Gaussian Process Regression (GPR) [18,19].

Machine learning (ML) models have gained much attention in recent years and have gradually become the third category of models. Given that machine learning is sometimes

differentiated from traditional statistics for its focus on prediction, it is not surprising that these methods are being applied to forecasting influenza. Traditional statistical models have a longstanding emphasis on inference, which is achieved through creating and fitting project-specific probability models. They are often less well-suited to data with large sample sizes and input variables [20]. By contrast, ML methods are data-driven and avoid making prior assumptions about underlying correlations and rather employ algorithms to identify patterns in the data [21,22]. In addition, ML methods are flexible in taking different types of input variables and a huge number of observations into consideration to improve predictive performance. The usage of some popular machine learning and deep learning methods in influenza forecasting has been discussed, such as Long Short Term Memory (LSTM) [23], Support Vector Machine (SVM) [24–27], and neural networks [28–31]. These methods show consistent and high forecasting accuracy but also suffer from the risk of over-fitting.

Many natural extreme phenomena, such as floods and earthquakes, are often described on an ordinal scale, but infectious disease incidence is usually described as a count or a percentage of a population. The use of the moving epidemic method is a notable exception, which is now routinely used to compare and communicate the current state of epidemics across nearby connected populations [32]. However, influenza forecasting has remained focused on non-ordinal target observations [33], limiting the range of analytical methods that can be applied.

Extreme Gradient Boosting (XGboost) is a decision-tree-based ensemble machine learning method employing the gradient boosting algorithm [34]. It has demonstrated good prediction performance on a wide range of problems in different industries, including finance, physics and clinical research (e.g. patient diagnosis) [35–38].

In this paper, we aim to construct an XGBoost model to make short-term predictions of the weekly influenza incidence as an ordinal variable, ranging from 1- to 4-week ahead of the

current time. We also evaluate the performance of XGBoost by accuracy metrics and compare it with baseline models.

## Methods

### *Data*

We used a global web-based collection tool for epidemiological indicators and data on influenza, Flu Informed Decisions (FluID) dataset from the World Health Organization (WHO) [39]. This platform collects weekly Influenza-Like Illness (ILI) incidence data from WHO member countries and regions, which is either submitted on a weekly basis or obtained by the WHO from regional networks such as EUROFlu [2].

The FluID data was available from ISO year 2010 week 1 to 2017 week 52 and included data from 146 countries initially. To ensure sufficient data for model training, countries with less than 50% of the data were excluded. Further countries that did not have at least 10 weeks of data for each year between 2010 and 2017 were also excluded. After applying these criteria were applied to the dataset, 32 countries remained, primarily in Europe and North America.

The key field in the data was ILI incidence, which was an integer ranging from 0 to 44965 (in week 52 of 2017 in the USA). This field was transformed into an ordinal variable by discretizing into N different bins with equal intervals, using N = 10 as the default. The highest incidence data for each country was used to add 10% as the upper boundary. The range from 0 to the upper limit was then divided into ten equal ordinal intervals, each of which was mapped to an ordinal value from 1 to 10, 1 represented the lowest incidence level, while 10 represented the highest level. Note that each country's classification was based on its own

influenza incidence level, so the same category in two different countries corresponded to different absolute levels of incidence.

## *Models*

We used XGBoost to establish a model to predict short-term weekly influenza incidence levels [34]. XGBoost is an implementation of the gradient-boosted decision trees and has been developed to improve computation speed and predictive performance for a variety of problems, including classification and regression [40]. Gradient boosting is an algorithm where new models are added in an adaptive way based on the residuals or errors of predictions from prior models and then combined to make the final prediction. Boosting is an ensemble method that creates a strong prediction model by iteratively combining a number of weak classifiers. New weak classifiers are added to correct the errors made by existing models, and every new model is added sequentially until no further improvements can be achieved or until a maximum number of models is added. Gradient boosting uses a gradient descent algorithm to minimize the loss when adding new models, i.e., at every optimization step, only models that reduce the residual or errors are added. XGBoost uses second-order Taylor expansion to minimize the loss function and added regularization terms to prevent overfitting.

To further validate the effectiveness of XGBoost for influenza forecasting, we constructed two additional baseline models for comparison: 1) null model, in which the prediction of the target week is the same as the most recent available observation week, and 2) historical average model in which the prediction of the target week is the average of observations of the same weeks in other years. The usual definition for historical average models is to mean value over prior observations for that week of the year [41]. Here, we use a slightly different categorical definition of the incidence level with the highest frequency across the same week in the other years in the study. The aim of the historical average model is similar to that of

the null model, which is to provide a baseline for comparison with the accuracy of the XGBoost model, reflecting how users might informally forecast the incidence levels for the next 1 to 4 weeks.

### *Forecast and features*

Our target was to predict ordinal categories for each week at the country level. We first did regular machine learning forecasting, in which we trained the model with a training set of fixed durations and then assessed the model's performance on a testing set. We designed our analysis to use 5 years of training data to predict one year of outcomes. The first training set used data from 2010 to 2014, the second training set used data from 2011 to 2015, and so on (S1 Table).

For predictors in the short-term forecasting model we used: categorical incidence levels of the prior  $n$  week and prior  $(n + 1)$  weeks, the month of the year (from January to December) and the season (spring, summer, autumn, and winter), where  $n$  represents the  $n$ -week ahead forecast. In a 1-week ahead forecast, the model uses the incidence levels of the prior 1 week and the prior 2 weeks; similarly, the incidence levels of the prior 4 weeks and prior 5 weeks will be used as predictors in the 4-week ahead prediction.

In addition to the fixed training window approach, we also trained the XGboost algorithm with an extending window. In the fixed window approach, we train the XGBoost model only once with the fixed training set and then predict the test set. Since the data were collected on a weekly basis, we are able to update our model by including the new coming data and retraining it to see if model performance can be improved. Thus we train the model with an extended training set for each week, which is called extending window approach in this paper. For example, if we are going to predict the week  $i$  ( $i > 2$ ) of the year 2015, our training set used data from 2010 until 2014 for all weeks and data from 2015 for weeks 1 to week  $(i - 1)$ . Our test data were data in 2015 week  $i$ . The baseline models were trained with



the fixed window approach only. Weeks with missing values for predictors were removed from both the training set and the test set.

XGBoost provides a large number of hyperparameters to help achieve optimal performance. They are mainly divided into three types, general parameters, booster parameters, and learning task parameters [42]. Booster parameters are closely related to the performance of the model, which is the focus of hyperparameter tuning. Grid search was used to find optimal values for hyperparameters max\_depth, min\_child\_weight, subsample, colsample\_bytree, learning rate and gamma. Grid search can be challenging and time-consuming due to the many parameters to optimize, even with XGBoost's rapid convergence. Our grid search for hyperparameters was carried out as below:

- 1) Firstly, find the optimal gamma and eta (learning rate) at the same time since they have an impact on the performance of the model. The values searched for gamma are 0.1, 0.2, 0.5, 1, 1.5, 2, and 10, while those for eta are 0.01, 0.02, 0.03, 0.06, 0.1, 0.2, and 0.3. We ran all possible combinations of these two hyperparameter values to tune, and the one with the best performance was selected as the optimal value for gamma and eta, respectively.
- 2) With the optimal values of gamma and eta obtained in the previous step, a grid search was conducted for max\_depth, and min\_child\_weight range from 0.1 to 1.
- 3) Made a grid-search over subsample and colsample\_bytree simultaneously range from 0.1 to 1.

K-fold cross-validation is used during the tuning process to assess the model's performance with different combinations of hyperparameter values. Since there is a dependency between weekly ILI incidence and future values that cannot be used to forecast past values, the traditional K-fold method that randomly splits the training set into K folds is not applicable to our data. Instead, we used cross-validation on an extending basis (S1 Fig). We selected data from 2010 to 2014 as the overall training set for the cross-validation, but during the process of rolling cross-validation,

we started with data from 2010 as the first fold of the training set and checked the accuracy of prediction for the data from 2011. Data from 2010 and 2011 then formed the second fold of the training set, and data from 2012 became the test for accuracy check. The accuracy metric used in the tuning process is macro-averaged mean absolute error (mMAE) which will be defined in detail later. This process was repeated until 2014 became the last test set. The final optimal values of the hyperparameter were given in S2 Table.

#### *Accuracy metrics*

We used two of the most commonly used metrics in ordinal classification problems [43], macro-averaged mean absolute error (mMAE) and mean zero-one error (MZE) ) to evaluate the model performance. Both metrics are defined as negatively oriented penalties that we aim to minimize: the lower the score, the better the forecast is considered.

#### Macro-averaged mean absolute error

Macro-averaged mean absolute error (mMAE) measure is adapted from the traditional class-based metric mean absolute error (MAE) which assesses the average deviation of the predicted class from the actual class, and it is defined as

$$MAE = \frac{1}{N} \sum_{i=1}^N |y_i^* - y_i|$$

where  $y_i$  and  $y_i^*$  denotes the true class and the predicted class respectively. However, MAE averages effectiveness across individual observations, which does not reflect the imbalanced distribution of classes in our datasets if many observations are in the lowest class and very few are in higher classes. Instead, we used macro-averaged mean absolute error (mMAE) as one of our metrics to assess the performance of our models in terms of predicting ordered outcomes. mMAE is obtained by first computing the MAE on a per-class

basis and then averaging the results across the classes so that mMAE is insensitive to class imbalance. Let  $y_i$  be the true class and  $y_i^*$  be the predicted class of  $i$ -th week in the test set. Let  $N_k$  be the number of true cases with the class  $k$  where  $k \in \{1, 2, \dots, 9, 10\}$ . There are 10 classes in our classification problem, i.e.,  $N_k = \sum_{i=1}^N I_{y_i=k}$  and  $N = \sum_{k=1}^{10} N_k$ . The Macro-averaged mean absolute error is calculated with the following formula:

$$mMAE = \frac{1}{10} \sum_{k=1}^{10} \frac{1}{N_k} \sum_{i=1}^N |y_i^* - y_i| I_{y_i=k}$$

, where

$$I_{y_i=k} = \begin{cases} 1, & \text{if } y_i = k \\ 0, & \text{if } y_i \neq k \end{cases}$$

### Mean zero-one error

Our second metric is the mean zero-one error (MZE) which is more frequently known as the error rate of classifiers and is, essentially, the proportion of time that a correct prediction is made

$$\begin{aligned} MZE &= \frac{1}{N} \sum_{i=1}^N I_{y_i^*=y_i} \\ &= 1 - Acc \end{aligned}$$

where

$$I_{y_i^*=y_i} = \begin{cases} 1, & \text{if } y_i^* = y_i \\ 0, & \text{if } y_i^* \neq y_i \end{cases}$$

$y_i$  and  $y_i^*$  denotes the true class and the predicted class respectively.  $Acc$  is the accuracy of the model, i.e., the number of correctly predicted categories divided by the total number of predictions. Therefore, MZE ranges between 0 and 1, and the lower the MZE, the higher accuracy indicates better predictive performance.

## Results

Country-level forecasts were performed using ILI data from 32 countries, located in northern temperate regions (S2 Fig). Due to the incompleteness of data, countries located outside of temperate regions were excluded from the analysis. The countries in the northern hemisphere's temperate regions demonstrated a similar trend in influenza activity, with ILI incidence typically rising at the end of the year and reaching a peak level at the beginning of the following year (Fig 1B). During the 2010 - 2017 surveillance, after excluding weeks with missing values, the data availability ranged between 229 and 417 weeks, with each country contributing an average of 337 weeks of data (median = 391 weeks). Of these weeks, over 60% fell into level 1, while 0.76% of the total weeks fell into levels 9 and 10 (Fig 1A).

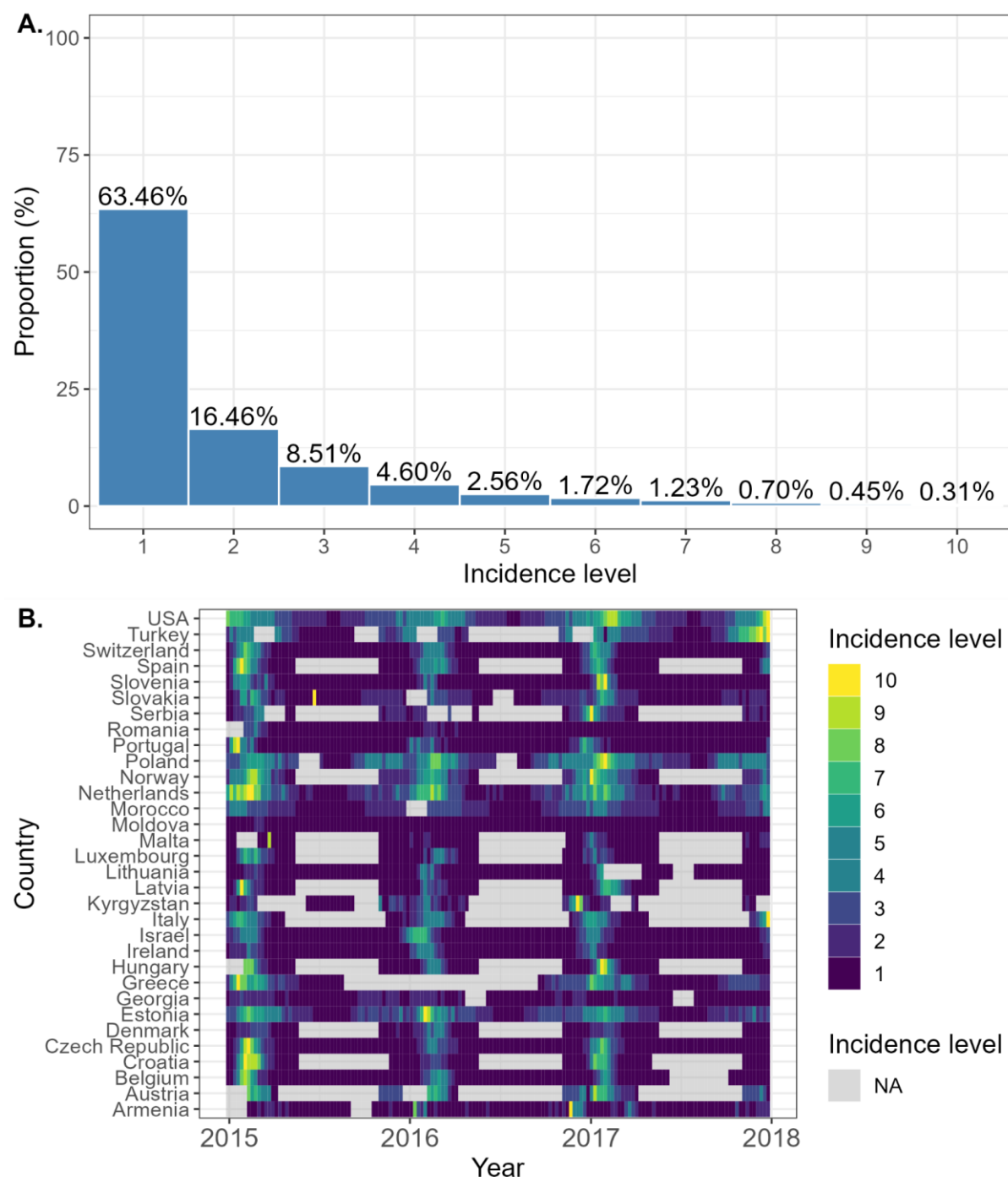


**Fig 1. Distribution of categorical incidence levels for weekly influenza-like illness for countries included in the study. A.** overall frequency of every level appearing in 32 countries. **B.** The heat map shows of incidence level in each country by time. Grey-shaded areas indicate that no available were data for those weeks.

## 254 *Predictive performance*

255 Overall, the XGBoost model with an extended window generated fewer errors and  
 256 demonstrated more stable predictive performance than the XGBoost model with a fixed  
 257 training window or the baseline models. The short-term prediction errors of different models  
 258 are summarized in Table 1, by averaging the mMAE is averaged across countries, and  
 259 presented for each prediction horizon (1-week ahead, 2-week ahead, etc. ). We separately  
 260 compare the mMAEs of three test periods (2015 to 2017). From Table 1, for these three test  
 261 periods, we show that prediction accuracy measured by mMAEs decreases with the  
 262 increasing forecast length (i.e. one to four-week in advance), but both XGBoost models (with  
 263 extending window and fixed window) uniformly outperform the two baseline models (Fig 2,  
 264 Table 1). In particular, the mMAEs of the XGBoost model with an extended window remain  
 265 below 1, on average across all countries, even as the forecast length increases, indicating  
 266 that, on average, the predicted classes are either correct or only one class away from the  
 267 true class. This XGBoost model has the lowest average MZEs for all prediction horizons  
 268 compared to the XGBoost model with a fixed window and baseline models (S3 Fig, S3  
 269 Table).

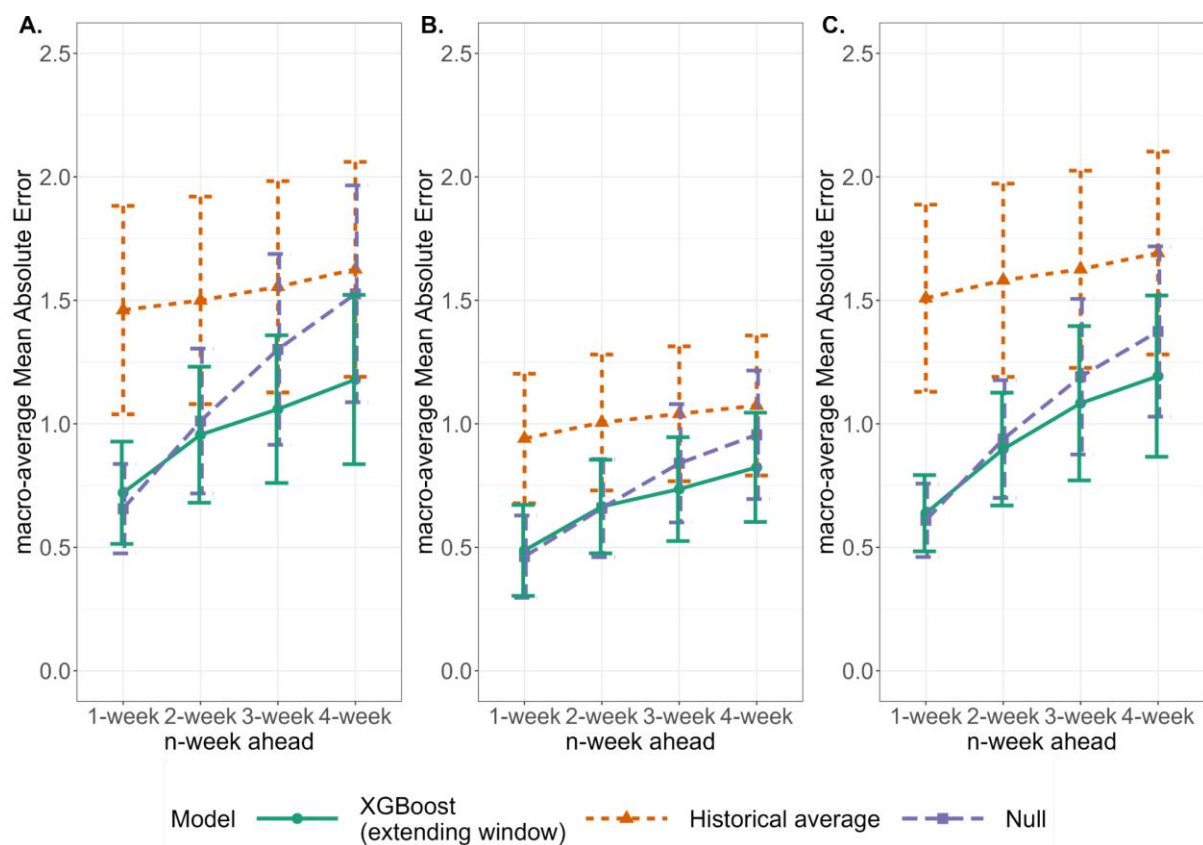


**Fig 2. Differences in macro-averaged mean absolute error (mMAE) by model.**

Comparison of mMAE for XGBoost (with an extended window) and baseline models while forecasting 1 to 4 weeks ahead. **A.** 2015, **B.** 2016, **C.** 2017.

**Table 1. Overall macro-averaged mean absolute error (mMAE) of XGboost compared with baseline models.** Overall mMAEs of 1- to 4-week ahead forecasts for each model are calculated as the average of 32 countries' mMAEs by year.

Year	Models	mMAE of n-week ahead			
		n = 1	n = 2	n = 3	n = 4
2015	XGBoost with extending window	0.721	0.956	1.060	1.179
	XGBoost with fixed window	0.822	0.997	1.102	1.221
	Historical average model	3.316	3.449	3.554	3.705
	Null model	2.908	1.848	2.447	2.908
2016	XGBoost with extending window	0.488	0.665	0.736	0.824
	XGBoost with fixed window	0.520	0.675	0.789	0.836
	Historical average model	3.338	3.200	3.270	3.247
	Null model	2.751	1.826	2.429	2.751
2017	XGBoost with extending window	0.638	0.898	1.084	1.193
	XGBoost with fixed window	0.645	0.918	1.148	1.268
	Historical average model	3.484	3.604	3.734	3.878
	Null model	2.663	1.720	2.221	2.663

The mMAEs for the extending window approach were consistently lower compared to the XGBoost model with a fixed window (Fig 3, Table 1). The mMAEs for the fixed window approach only remained below 1 for 1- to 4-week forecasts in 2016, but exceeded 1 for 3- and 4-week ahead forecasts in 2015 and 2017. Although the two XGBoost models had similar MZEs, the extending window approach still resulted in a lower MZE for each prediction horizon (S4 Fig, S3 Table). The better performance of the extending window approach can be attributed to its continuous addition of the predicted weeks' observations to the training set, allowing the model to learn more data, resulting in smaller prediction errors.



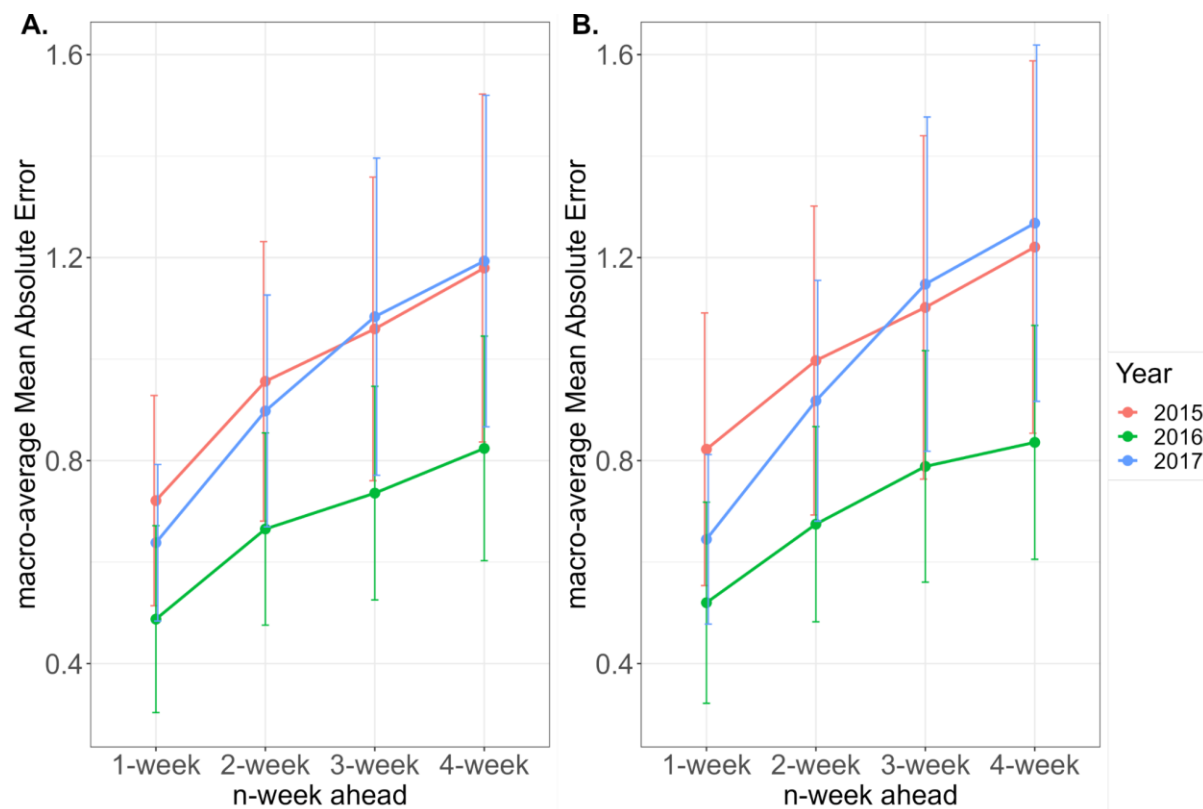


**Fig 3. Macro-averaged mean absolute error (mMAE) of XGBoost models.** Comparison of mMAEs for weekly forecasting ranging from 1-to 4-week ahead for the years 2015 to 2017. **A.** The XGBoost model with an extended window approach. **B.** The XGBoost model with a fixed window approach.

There is substantial variation in the prediction accuracy, as indicated by mMAE, among the countries (Fig 4, S4 – S6 Table). For instance, Moldova, had remarkably low mMAEs from 2015 to 2017, even achieving 0 in 2016 and 2017. Conversely, certain countries, such as Hungary and Norway, consistently exhibit much higher mMAEs compared to other countries. Similar results were found for MZEs (S5 Fig, S7 – S9 Table). The performance of XGBoost on the test set can be affected mainly by the quality of training data. By checking the missing data for countries, we discover that countries with high mMAEs often have more incomplete data than better-performing countries, implying that they have a smaller sample size of training sets, failing to capture complex epidemic patterns of influenza (Fig 2B).

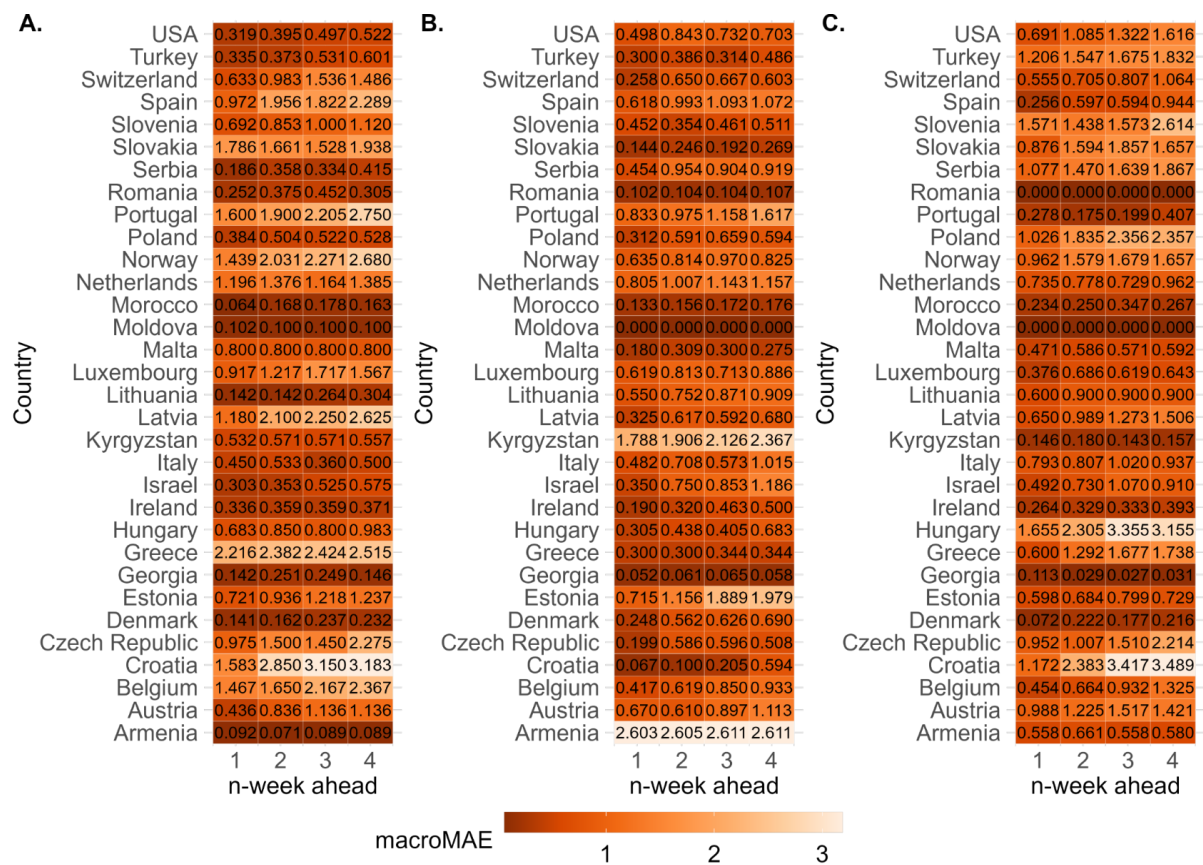


**Fig 4. Macro-averaged mean absolute error (mMAE) for 32 countries.** mMAEs of predictions by the XGBoost model with an extended window for the year **A.** 2015. **B.** 2016. and **C.** 2017.

We investigated the influenza distribution and forecasts over a 3-year period in four countries selected based on their mMAEs and data completeness and found different qualitative drivers of accuracy. The plots in Fig 5 compare the predicted values from four models with actual data for 1 to 4-week-ahead forecasts in Moldova, Switzerland, Estonia and Hungary separately. Moldova had the lowest mMAE, but its influenza activity barely fluctuated with 97.5% (390 out of 400 weeks) of the weeks remaining at level 1. Conversely, Switzerland and Estonia had 25.3% (82 out of 406 weeks) and 72.5% (290 out of 400 weeks) of the weeks, respectively, above the baseline level. All four models successfully predict peak influenza season for 1-week and 2-week ahead forecasts in 2015 and 2016 in

Switzerland Estonia, but the historical average model failed to identify peaks for 3-week and 4-week ahead forecasts. The other three models could identify peaks up to 4-week ahead of forecasts, with the XGboost with extending approach being the most accurate. The deviation between actual observation and prediction is typically high when there is a sudden increase or decrease in flu incidence levels. In Hungary, due to the limited sample size of the training set and the complexities of influenza activity, a large deviation between actual observation and prediction even for the 1-week forward forecast. The prediction of XGboost with an extending window provided the closest prediction to the observed peak (Fig 6).

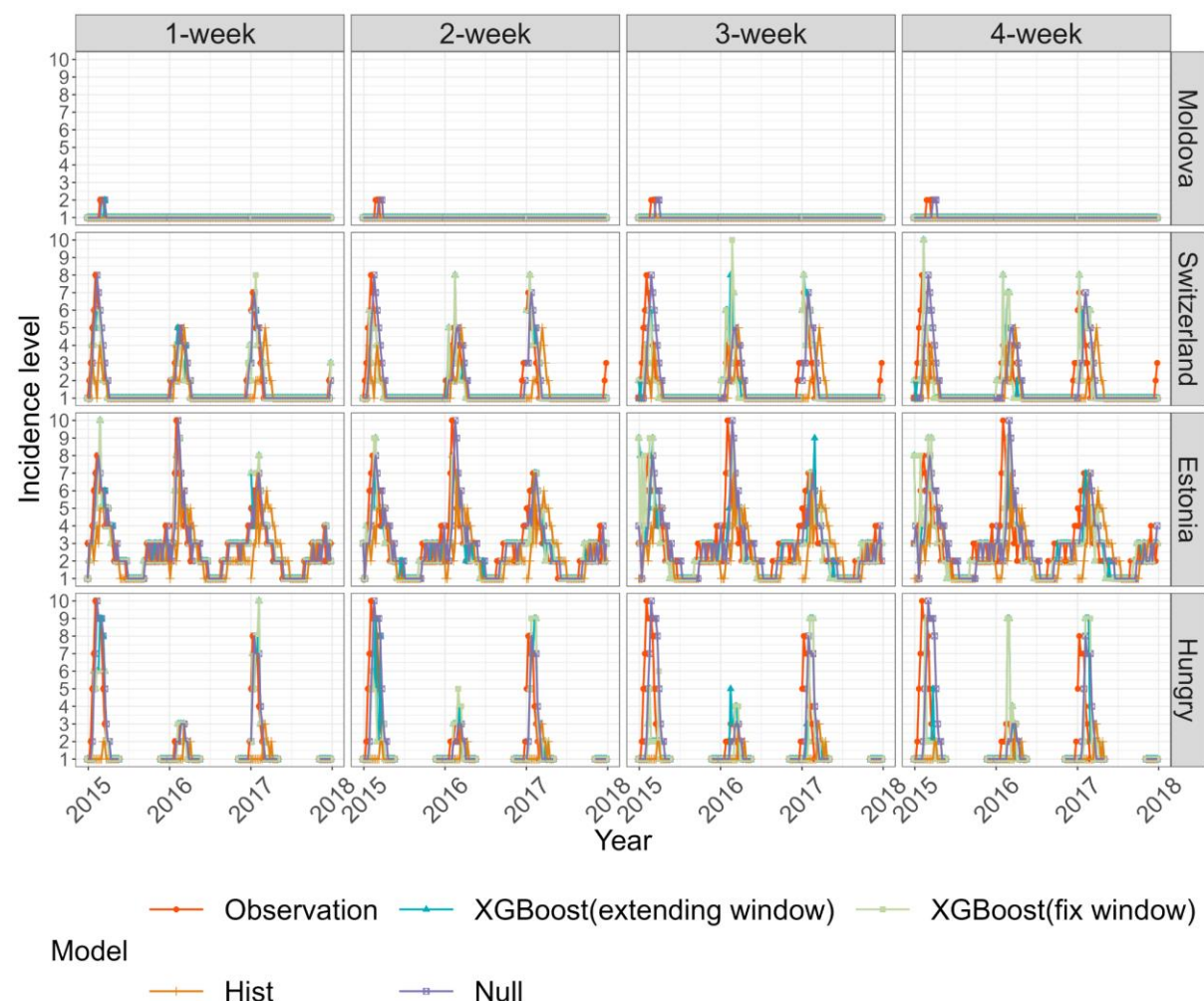


**Fig 5. Comparison of Actual and predicted incidence by country.** Countries Moldova, Switzerland, Estonia and Hungary are selected. Models include the two XGBoost models, the historical average model and the null model while forecasting 1- to 4-week ahead for the test period year 2015 to 2017.

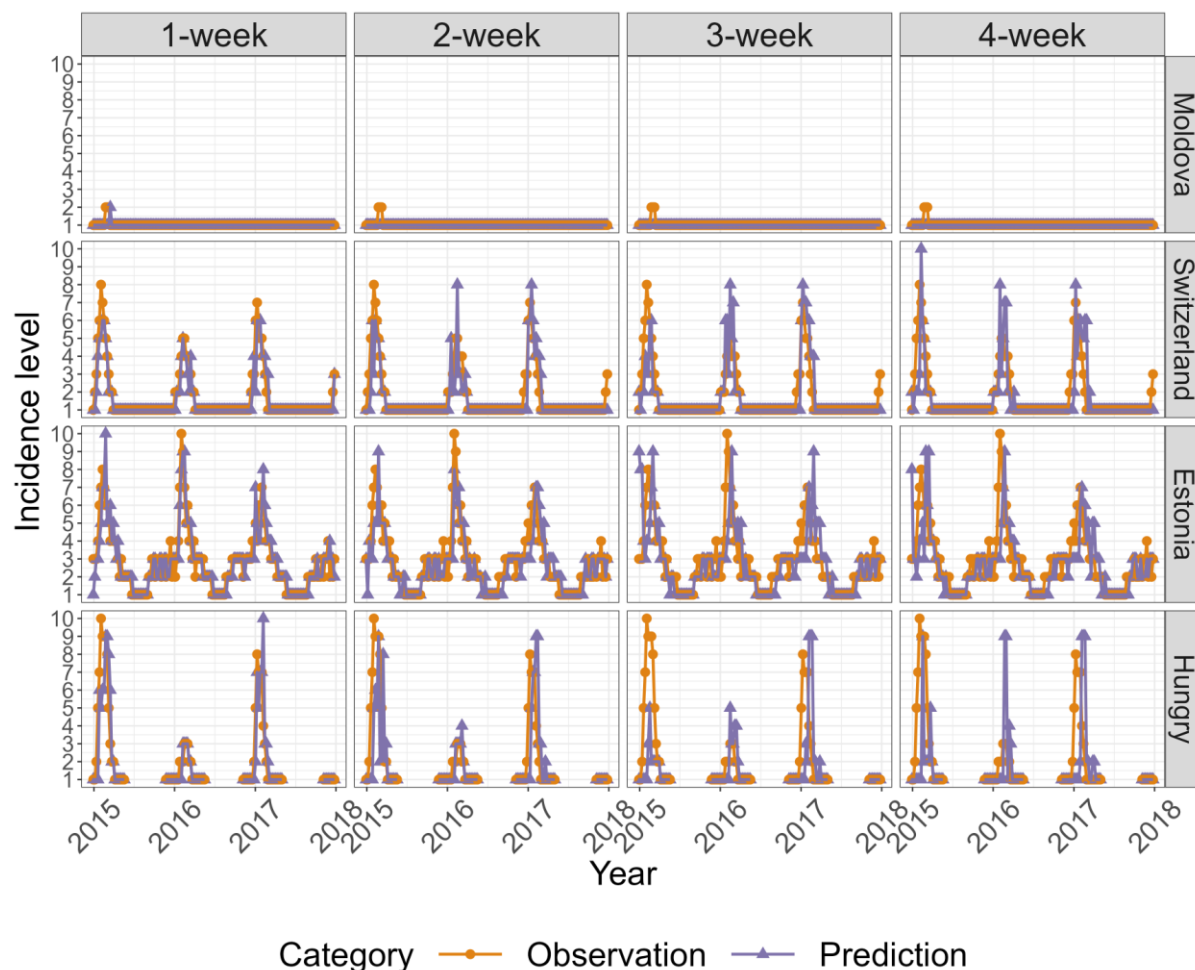


**Fig 6. Comparison of actual and predicted incidence.** Predicted incidences are generated by the XGBoost model with an extended window for Moldova, Switzerland, Estonia and Hungary; for forecasts 1 to 4 weeks ahead for the test period year 2015 to 2017.

## Discussion

In this work, we have proposed a potential machine learning model for influenza forecasting using a 10-unit ordinal variable to describe the case incidence. We evaluated two XGBoost machine learning models, one with a fixed window training set and the other with an extended window training set, and compared them to baseline models. We measured their accuracy using the mean zero-one error (MZE) and macro-averaged mean absolute error (mMAE). Our results showed that both XGBoost models outperformed the baseline models, with the extended window XGBoost model consistently achieving the highest accuracy.

This framework is novel because we defined the outcome on an ordinal scale, which is often how influenza incidence is communicated[32]. However, our results are not directly comparable to other forecasting studies, and the XGBoost model has not been validated against other data sources. This highlights the need to test its applicability in real-world public health practice.

The use of a categorical outcome enabled us to apply machine learning algorithms. Although the XGBoost has advantages, it has not been tested against other data sources. Machine learning algorithms' performance can be limited by the quality of the training and testing data, and inconsistencies between different databases may reduce the generalisability of the XGBoost prediction model [44]. Further testing is needed to determine the applicability of the in real-world public health practice.

Our baseline models provide a basic framework for assessing the potential of machine learning forecasts. The baseline models are intended to reflect the most basic of implicit forecast assumptions: they assume that incidence will remain unchanged and revert to its historical average. Our methods offer improvements over these assumptions, for example, the 4-week forecast horizon XGBoost model with an extended window being more accurate

than assuming the incidence would follow the historical average and more accurate than the default 1-week ahead model with no change assumption.

This work has several limitations. One of the challenges in working with infectious disease datasets is the limited period of data available for model estimation and evaluation, compared to other datasets used in machine learning. For each country in the study, only 5 years of data were used for model training, leaving only 3 years for testing. Cross-validation was used to find the optimal hyperparameters instead of using an independent validation set. Additionally, countries with fewer weeks of data in the training set tend to have higher prediction errors, which suggests that accuracy will improve as more data becomes available. Furthermore, the results should be interpreted with caution, given the disruption to influenza transmission during the COVID-19 pandemic, as patterns may change as the transmission is re-established.

Our forecasts showed reduced accuracy in predicting turning points of the epidemic (Fig 7). When there is a sudden increase in incidence levels, they are often underestimated. On the other hand, a sudden decrease in incidence levels results in them being easily overestimated. This is especially important in a public health context where accurately predicting rare cases of much higher than usual incidence levels or earlier or later ends of the epidemic is crucial. Thus, improving the prediction stability at the extreme points of season patterns remains a priority in ongoing forecasting work.



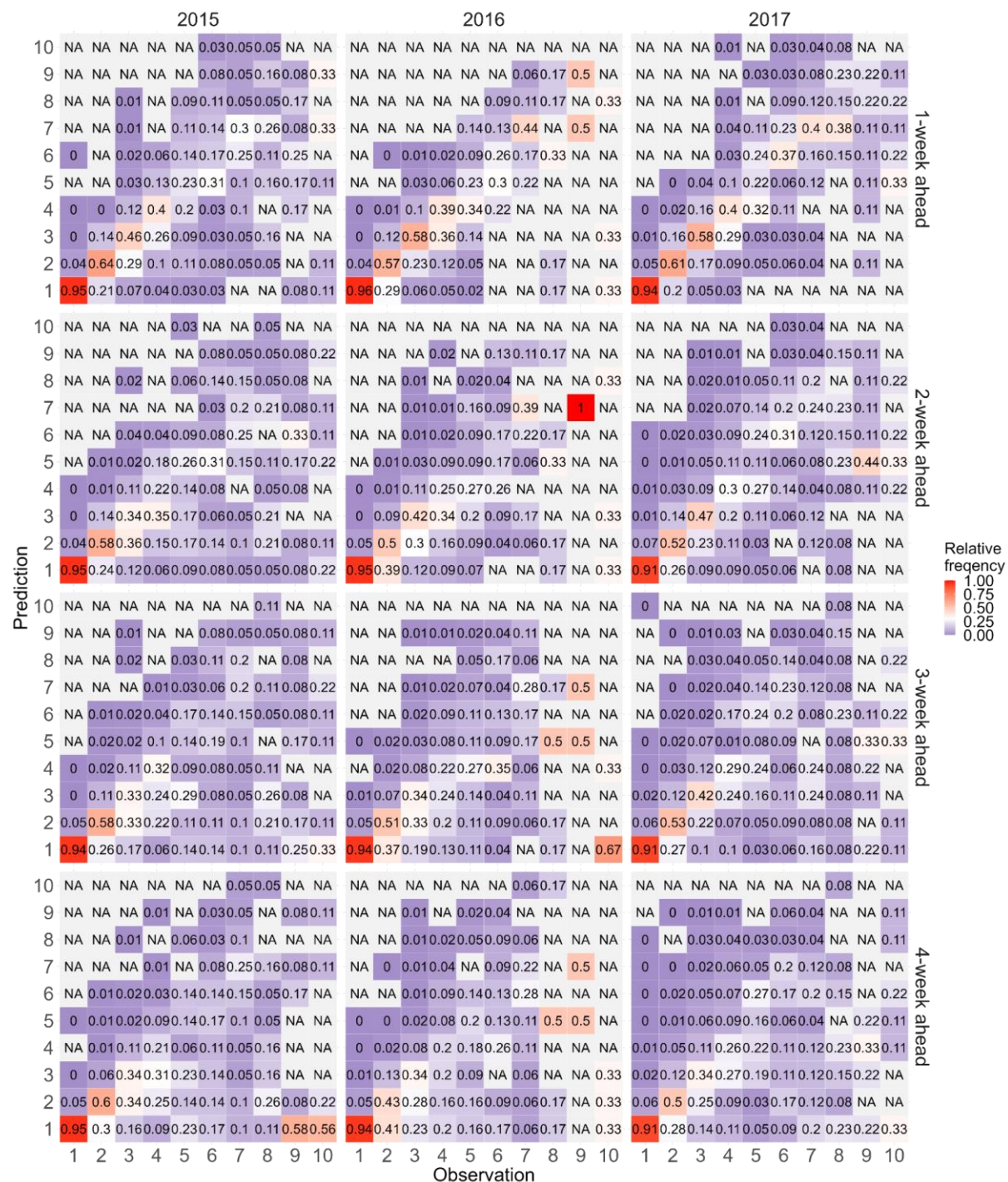


**Fig 7. Distribution of predictions against each decile of observation for the XGBoost model with an extended window.** Rows of heat maps are ordered from 1 week ahead (top) to 4 weeks ahead (bottom). Columns of heat maps are ordered from 2015 (left) to 2017

(right). Values on the diagonal are the accuracy of forecasts, while other values represent the frequency at each level that was incorrectly predicted to be the other level.

## Conclusion

Forecasting influenza as an ordinal outcome is a feasible task for machine learning. The widely used XGBoost model, even with a limited set of features, provides significantly more accurate predictions than the standard baseline models. With datasets that have longer history and comprehensive spatial coverage, it is possible to achieve more accurate forecasts. Similar to other epidemiological models, the framework can easily be expanded to include population serology and population mobility [45] or other relevant features as more data become available [46].



395 **Supporting information**

396 **S1 Table. Time ranges of training and test sets.**

397 (XLSX)

398 **S2 Table. Summary of optimal values of hyperparameters for XGBoost models.**

399 (XLSX)

400 **S3 Table. Overall mean-zero error (MZE) of XGboost compared with baseline models.**

401 Overall MZEs of 1- to 4-week ahead forecasts for each model are calculated as the average  
402 of 32 countries' MZEs by year.

403 (XLSX)

404 **S4 Table. Macro-average mean absolute error (mMAE) for the prediction by country in**  
405 **2015.**

406 (XLSX)

407 **S5 Table. Macro-average mean absolute error (mMAE) for the prediction by country**  
408 **in 2016.**

409 (XLSX)

410 **S6 Table. Macro-average mean absolute error (mMAE) for the prediction by country**  
411 **in 2017.**

412 (XLSX)

413 **S7 Table. Mean-zero error (MZE) for the prediction by country in 2015.**

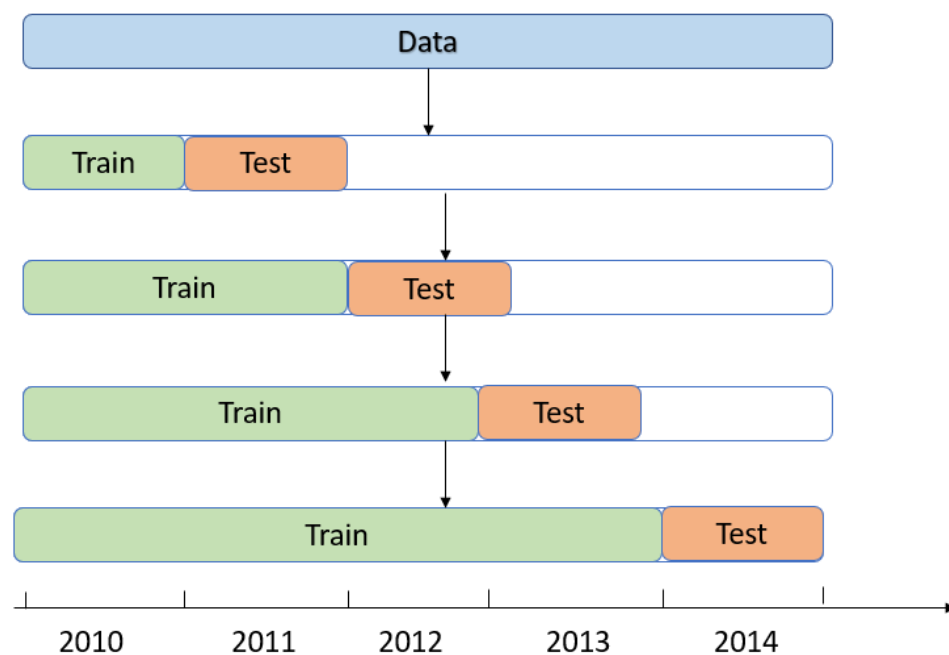
414 (XLSX)

415 **S8 Table. Mean-zero error (MZE) for the prediction by country in 2016.**

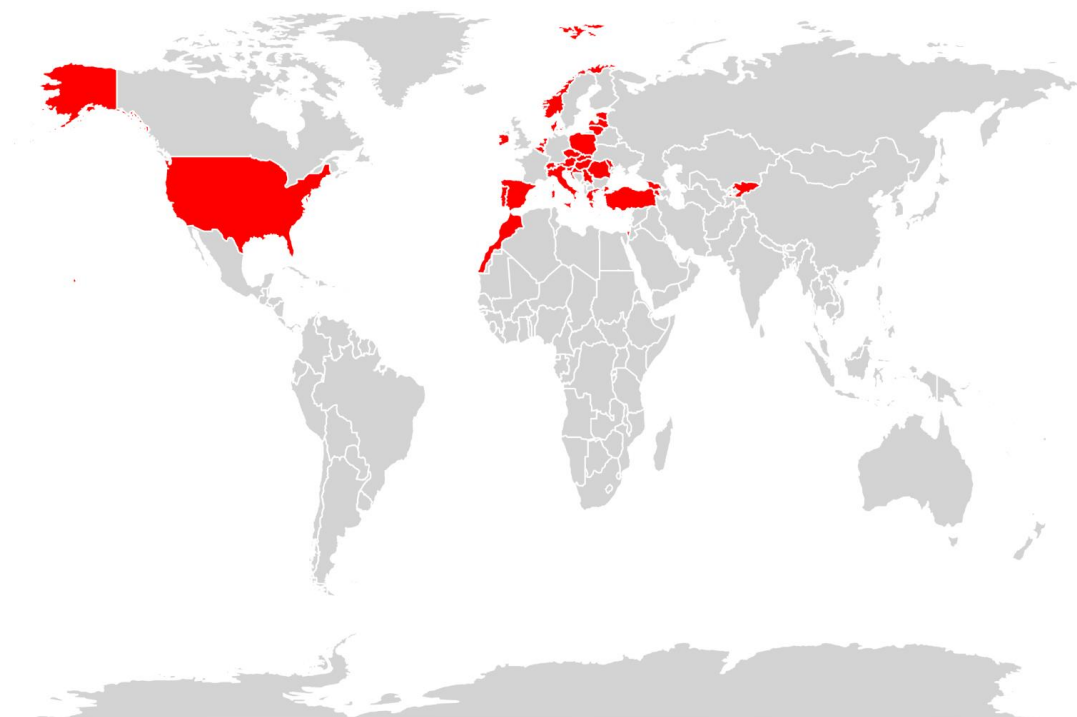
416 (XLSX)

417 **S9 Table. Mean-zero error (MZE) for the prediction by country in 2017.**

418 (XLSX)

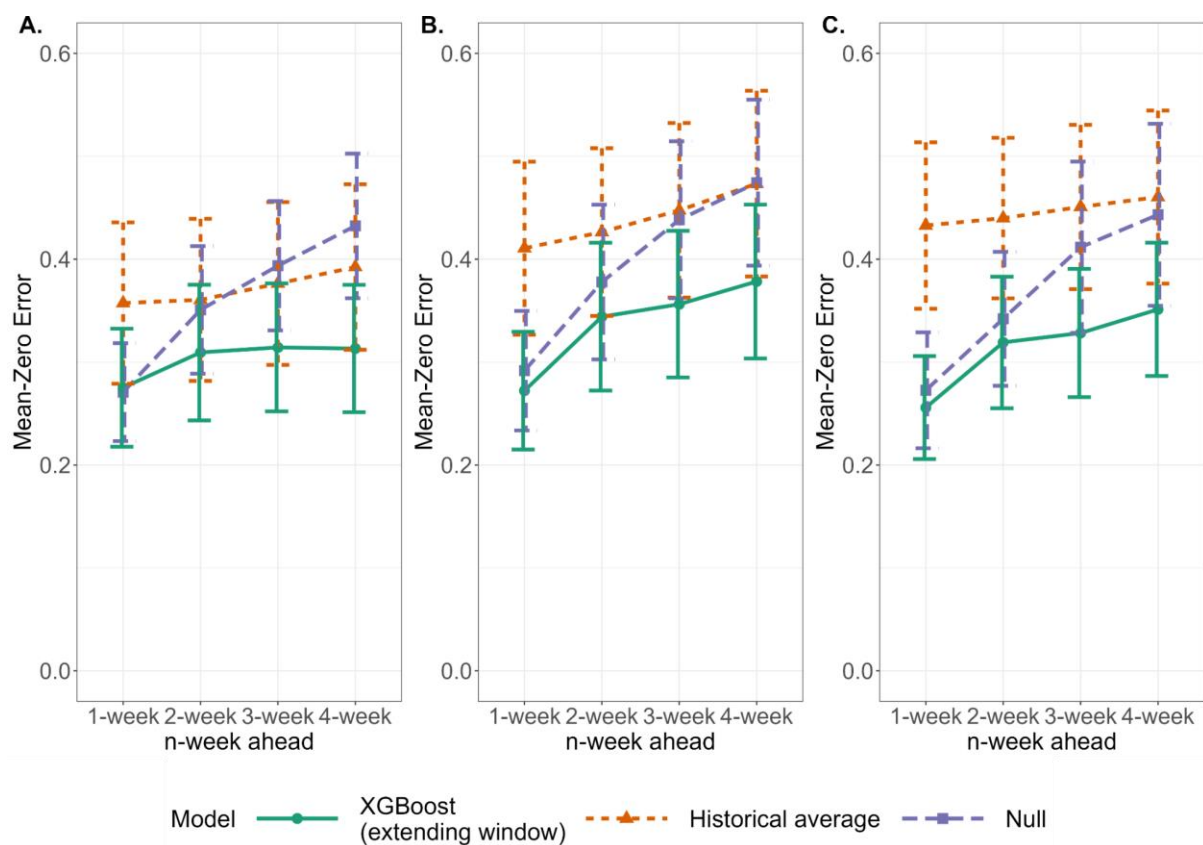


**S1 Fig. Time series split cross-validation.**

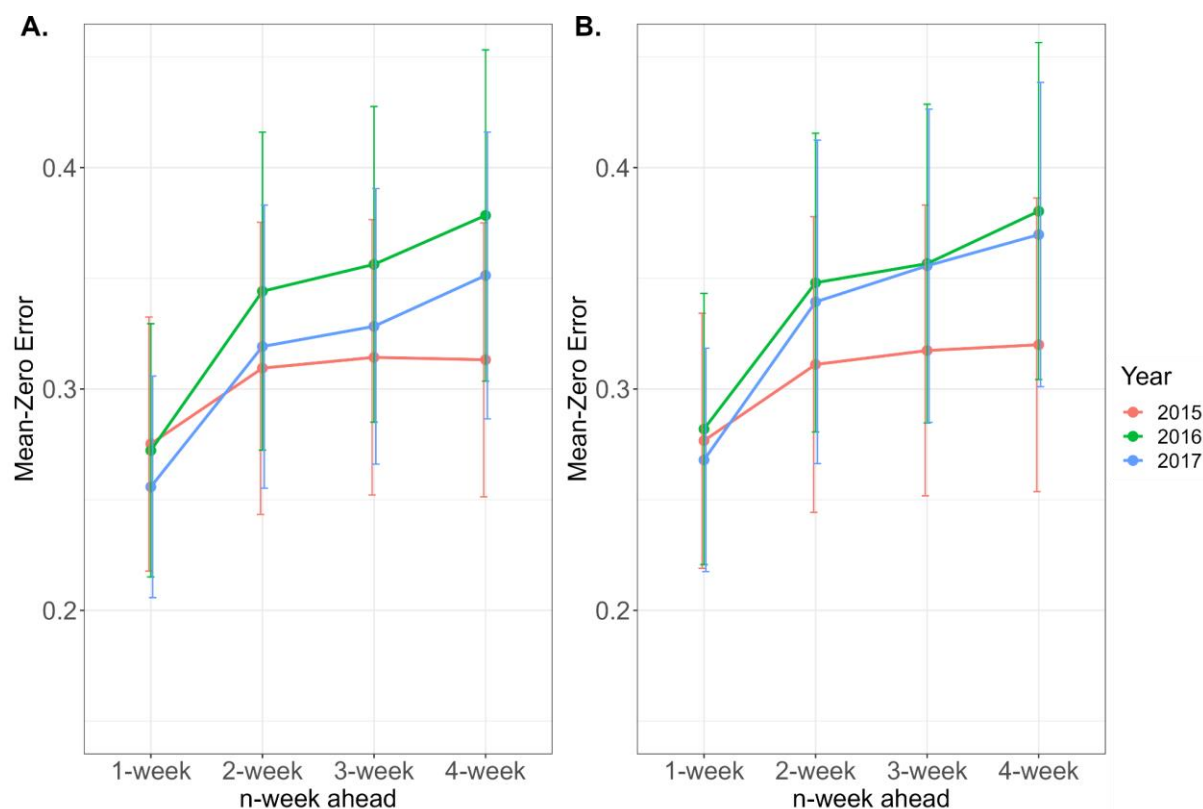


421

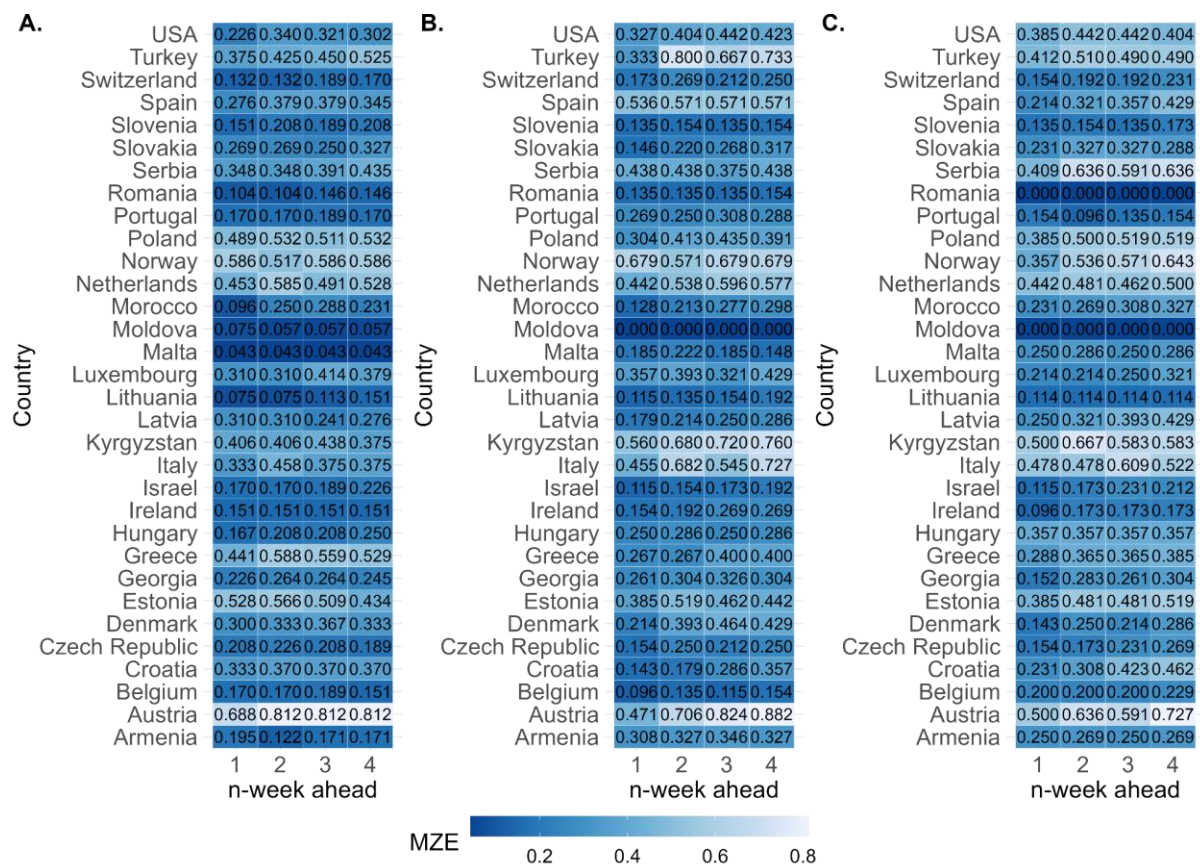
422 **S2 Fig. World map.** 32 Countries included in this study are marked in red. Samples are  
 423 mainly from North America and Europe.



**S3 Fig. Differences in mean-zero error (MZE) by model.** Comparison of mean-zero error (MZE) for XGBoost (with an extended window approach) and baseline models while forecasting 1 to 4 weeks ahead for the test period year 2015 to 2017.



**S4 Fig. Mean-zero error (MZE) of XGBoost models.** Comparison of MZEs for weekly forecasting ranging from 1- to 4-week ahead in 2015 to 2017. **A.** The XGBoost model with an extended approach. **B.** The XGBoost model with a fixed window approach.



**S5 Fig. Mean-zero error (MZE) for 32 countries.** MZEs of predictions by the XGBoost model with an extended window for the year **A.** 2015. **B.** 2016. and **C.** 2017.

## 436 **Acknowledgements**

437 The authors acknowledge funding from the MRC Centre for Global Infectious Disease  
 438 Analysis (MR/R015600/1), jointly funded by the UK Medical Research Council (MRC) and  
 439 the UK Foreign, Commonwealth & Development Office (FCDO), under the MRC/FCDO  
 440 Concordat agreement, and also part of the EDCTP2 programme supported by the European  
 441 Union. S.R. acknowledges the support from Wellcome Trust Investigator Award (UK,  
 442 200861/Z/16/Z). KOK acknowledges funding from HMRF (INF-CUHK-1).

## 443 **Author Contributions**

444 **Conceptualization:** Haowei Wang, Steven Riley

445 **Data curation:** Haowei Wang

446 **Formal analysis:** Haowei Wang

447 **Funding acquisition:**

448 **Methodology:** Haowei Wang

449 **Software:** Haowei Wang

450 **Supervision:** Steven Riley

451 **Validation:** Haowei Wang

452 **Visualization:** Haowei Wang

453 **Writing – original draft:** Haowei Wang

454 **Writing – review & editing:** Haowei Wang, Steven Riley, Kin On Kwok

455



## References

1. Influenza (Seasonal). [cited 9 Mar 2022]. Available: [https://www.who.int/en/news-room/fact-sheets/detail/influenza-\(seasonal\)](https://www.who.int/en/news-room/fact-sheets/detail/influenza-(seasonal))
2. Global\_Influenza\_Strategy\_2019\_2030\_Summary\_English.pdf. Available: [https://www.who.int/influenza/Global\\_Influenza\\_Strategy\\_2019\\_2030\\_Summary\\_English.pdf](https://www.who.int/influenza/Global_Influenza_Strategy_2019_2030_Summary_English.pdf)
3. Viboud C, Vespignani A. The future of influenza forecasts. *Proceedings of the National Academy of Sciences of the United States of America*. 2019. pp. 2802–2804.
4. Ali ST, Cowling BJ. Influenza Virus: Tracking, Predicting, and Forecasting. *Annu Rev Public Health*. 2021;42: 43–57.
5. Chretien J-P, George D, Shaman J, Chitale RA, McKenzie FE. Influenza forecasting in human populations: a scoping review. *PLoS One*. 2014;9: e94130.
6. Nsoesie EO, Brownstein JS, Ramakrishnan N, Marathe MV. A systematic review of studies on forecasting the dynamics of influenza outbreaks. *Influenza Other Respi Viruses*. 2014;8: 309–316.
7. Brooks LC, Farrow DC, Hyun S, Tibshirani RJ, Rosenfeld R. Nonmechanistic forecasts of seasonal influenza with iterative one-week-ahead distributions. *PLoS Comput Biol*. 2018;14: e1006134.
8. Yang W, Lau EHY, Cowling BJ. Dynamic interactions of influenza viruses in Hong Kong during 1998–2018. *PLoS Comput Biol*. 2020;16: e1007989.
9. Kramer SC, Shaman J. Development and validation of influenza forecasting for 64 temperate and tropical countries. *PLoS Comput Biol*. 2019;15: e1006742.
10. Shaman J, Karspeck A, Yang W, Tamerius J, Lipsitch M. Real-time influenza forecasts during the 2012–2013 season. *Nat Commun*. 2013;4: 1–10.
11. Kermack WO, McKendrick AG, Walker GT. A contribution to the mathematical theory of epidemics. *Proceedings of the Royal Society of London Series A, Containing Papers of a Mathematical and Physical Character*. 1927;115: 700–721.
12. Laskowski M, Demianyk BCP, Witt J, Mukhi SN, Friesen MR, McLeod RD. Agent-based modeling of the spread of influenza-like illness in an emergency department: a simulation study. *IEEE Trans Inf Technol Biomed*. 2011;15: 877–889.
13. Arduin H, Domenech de Cellès M, Guillemot D, Watier L, Opatowski L. An agent-based model simulation of influenza interactions at the host level: insight into the influenza-related burden of pneumococcal infections. *BMC Infect Dis*. 2017;17: 382.
14. Dugas AF, Jalalpour M, Gel Y, Levin S, Torcaso F, Igusa T, et al. Influenza forecasting with Google Flu Trends. *PLoS One*. 2013;8: e56176.
15. Spaeder MC, Stroud JR, Song X. Time-series model to predict impact of H1N1 influenza on a children's hospital. *Epidemiol Infect*. 2012;140: 798–802.

- 493 16. Achrekar H, Gandhe A, Lazarus R, Yu S-H, Liu B. Predicting Flu Trends using Twitter  
494 data. 2011 IEEE Conference on Computer Communications Workshops (INFOCOM  
495 WKSHPS). 2011. pp. 702–707.
- 496 17. Perrotta D, Tizzoni M, Paolotti D. Using Participatory Web-based Surveillance Data to  
497 Improve Seasonal Influenza Forecasting in Italy. Proceedings of the 26th International  
498 Conference on World Wide Web. Republic and Canton of Geneva, CHE: International  
499 World Wide Web Conferences Steering Committee; 2017. pp. 303–310.
- 500 18. Chen S, Xu J, Wu Y, Wang X, Fang S, Cheng J, et al. Predicting temporal propagation  
501 of seasonal influenza using improved gaussian process model. J Biomed Inform.  
502 2019;93: 103144.
- 503 19. Predicting Spatio–Temporal Propagation of Seasonal ...Predicting Spatio-Temporal  
504 Propagation of Seasonal. <https://www.aaai.org> › AAAI16 › paper ›  
505 download<https://www.aaai.org> › AAAI16 › paper › download<https://ojs.aaai.org> ›  
506 index.php › AAAI › article › view<https://ojs.aaai.org> › index.php › AAAI › article › view.  
507 Available:  
508 <https://www.aaai.org/ocs/index.php/AAAI/AAAI16/paper/download/11998/12177>
- 509 20. Bzdok D, Altman N, Krzywinski M. Statistics versus machine learning. Nat Methods.  
510 2018;15: 233–234.
- 511 21. Bzdok D. Classical Statistics and Statistical Learning in Imaging Neuroscience. Front  
512 Neurosci. 2017;11: 543.
- 513 22. Bzdok D, Krzywinski M, Altman N. Points of Significance: Machine learning: a primer.  
514 Nat Methods. 2017;14: 1119–1120.
- 515 23. Venna SR, Tavanaei A, Gottumukkala RN, Raghavan VV, Maida AS, Nichols S. A  
516 Novel Data-Driven Model for Real-Time Influenza Forecasting. IEEE Access. undefined  
517 2019;7: 7691–7701.
- 518 24. A SVM-based prediction method for H5N1 Avian Influenza.  
519 <https://citeseerx.ist.psu.edu> › viewdoc › download<https://citeseerx.ist.psu.edu> › viewdoc ›  
520 download. Available:  
521 [https://citeseerx.ist.psu.edu/viewdoc/download?doi=10.1.1.842.4765&rep=rep1&type=p](https://citeseerx.ist.psu.edu/viewdoc/download?doi=10.1.1.842.4765&rep=rep1&type=pdf)  
522 [df](https://citeseerx.ist.psu.edu/viewdoc/download?doi=10.1.1.842.4765&rep=rep1&type=pdf)
- 523 25. Nsoesie EO, Oladeji O, Abah ASA, Ndeffo-Mbah ML. Forecasting influenza-like illness  
524 trends in Cameroon using Google Search Data. Sci Rep. 2021;11: 1–11.
- 525 26. Liang F, Guan P, Wu W, Huang D. Forecasting influenza epidemics by integrating  
526 internet search queries and traditional surveillance data with the support vector machine  
527 regression model in Liaoning, from 2011 to 2015. PeerJ. 2018;6: e5134.
- 528 27. Singh S, Kaur H. Influenza prediction from social media texts using machine learning. J  
529 Phys Conf Ser. 2021;1950: 012018.
- 530 28. Wu Y. DL4Epi: Deep Learning for Epidemiological Predictions. Github;  
531 doi:10.1145/3209978.3210077
- 532 29. Aiken EL, Nguyen AT, Viboud C, Santillana M. Toward the use of neural networks for  
533 influenza prediction at multiple spatial resolutions. Sci Adv. 2021;7.

doi:10.1126/sciadv.abb1237

30. Li Z, Luo X, Wang B, Bertozzi AL, Xin J. A Study on Graph-Structured Recurrent Neural Networks and Sparsification with Application to Epidemic Forecasting. *Optimization of Complex Systems: Theory, Models, Algorithms and Applications*. Springer International Publishing; 2020. pp. 730–739.
31. Hu H, Wang H, Wang F, Langley D, Avram A, Liu M. Prediction of influenza-like illness based on the improved artificial tree algorithm and artificial neural network. *Sci Rep*. 2018;8: 4895.
32. Vega T, Lozano JE, Meerhoff T, Snacken R, Mott J, Ortiz de Lejarazu R, et al. Influenza surveillance in Europe: establishing epidemic thresholds by the moving epidemic method. *Influenza Other Respi Viruses*. 2013;7: 546–558.
33. Reich NG, Brooks LC, Fox SJ, Kandula S, McGowan CJ, Moore E, et al. A collaborative multiyear, multimodel assessment of seasonal influenza forecasting in the United States. *Proc Natl Acad Sci U S A*. 2019;116: 3146–3154.
34. Chen T, Guestrin C. XGBoost: A Scalable Tree Boosting System. *Proceedings of the 22nd ACM SIGKDD International Conference on Knowledge Discovery and Data Mining*. New York, NY, USA: Association for Computing Machinery; 2016. pp. 785–794.
35. Wang J, Cheng Q, Dong Y. An XGBoost-based multivariate deep learning framework for stock index futures price forecasting. *Kybernetes*. 2022;ahead-of-print. doi:10.1108/K-12-2021-1289
36. Qin R. The Construction of Corporate Financial Management Risk Model Based on XGBoost Algorithm. *Journal of Mathematics*. 2022;2022. doi:10.1155/2022/2043369
37. Zhang X-X, Deng T, Jia G-Z. Nuclear spin-spin coupling constants prediction based on XGBoost and LightGBM algorithms. *Mol Phys*. 2020;118: e1696478.
38. Ogunleye A, Wang Q-G. XGBoost Model for Chronic Kidney Disease Diagnosis. *IEEE/ACM Trans Comput Biol Bioinform*. 2020;17: 2131–2140.
39. FluID. [cited 28 Jul 2022]. Available: <https://www.who.int/teams/global-influenza-programme/surveillance-and-monitoring/fluid>
40. demo at master · dmlc/xgboost. Github; Available: <https://github.com/dmlc/xgboost>
41. Forecasting: Principles and Practice (2nd ed). [cited 30 Sep 2022]. Available: <https://otexts.com/fpp2/>
42. XGBoost Parameters — xgboost 2.0.0-dev documentation. [cited 3 Nov 2022]. Available: <https://xgboost.readthedocs.io/en/latest/parameter.html>
43. Baccianella S, Esuli A, Sebastiani F. Evaluation Measures for Ordinal Regression. 2009 Ninth International Conference on Intelligent Systems Design and Applications. 2009. pp. 283–287.
44. Jain A, Patel H, Nagalapatti L, Gupta N, Mehta S, Guttula S, et al. Overview and Importance of Data Quality for Machine Learning Tasks. *Proceedings of the 26th ACM SIGKDD International Conference on Knowledge Discovery & Data Mining*. New York,

- 573 NY, USA: Association for Computing Machinery; 2020. pp. 3561–3562.
- 574 45. Liang J-B, Yuan H-Y, Li K-K, Wei W-I, Wong SYS, Tang A, et al. Path to normality:  
 575 Assessing the level of social-distancing measures relaxation against antibody-resistant  
 576 SARS-CoV-2 variants in a partially-vaccinated population. *Comput Struct Biotechnol J*.  
 577 2022;20: 4052–4059.
- 578 46. Kwok KO, Cowling B, Wei V, Riley S, Read JM. Temporal variation of human  
 579 encounters and the number of locations in which they occur: a longitudinal study of  
 580 Hong Kong residents. *J R Soc Interface*. 2018;15. doi:10.1098/rsif.2017.0838